

Journal Pre-proofs

Design, synthesis and biological research of novel *N*-phenylbenzamide-4-methylamine acridine derivatives as potential topoisomerase I/II and apoptosis-inducing agents

Bin Zhang, Zhende Dou, Zheng Xiong, Ning Wang, Shan He, Xiaojun Yan, Haixiao Jin

PII: S0960-894X(19)30672-9
DOI: <https://doi.org/10.1016/j.bmcl.2019.126714>
Reference: BMCL 126714

To appear in: *Bioorganic & Medicinal Chemistry Letters*

Received Date: 27 August 2019
Revised Date: 18 September 2019
Accepted Date: 19 September 2019

Please cite this article as: Zhang, B., Dou, Z., Xiong, Z., Wang, N., He, S., Yan, X., Jin, H., Design, synthesis and biological research of novel *N*-phenylbenzamide-4-methylamine acridine derivatives as potential topoisomerase I/II and apoptosis-inducing agents, *Bioorganic & Medicinal Chemistry Letters* (2019), doi: <https://doi.org/10.1016/j.bmcl.2019.126714>

This is a PDF file of an article that has undergone enhancements after acceptance, such as the addition of a cover page and metadata, and formatting for readability, but it is not yet the definitive version of record. This version will undergo additional copyediting, typesetting and review before it is published in its final form, but we are providing this version to give early visibility of the article. Please note that, during the production process, errors may be discovered which could affect the content, and all legal disclaimers that apply to the journal pertain.

© 2019 Elsevier Ltd. All rights reserved.



**Design, synthesis and biological research of novel
N-phenylbenzamide-4-methylamine acridine derivatives as potential
topoisomerase I/II and apoptosis- inducing agents**

Bin Zhang ^a, Zhende Dou ^a, Zheng Xiong ^a, Ning Wang ^{b,*}, Shan He ^a, Xiaojun Yan ^a,
Haixiao Jin ^{a,**}

^a Li Dak Sum Yip Yio Chin Kenneth Li Marine Biopharmaceutical Research Center,
Department of Marine Pharmacy, College of Food and Pharmaceutical Sciences,
Ningbo University, Ningbo, Zhejiang, 315800, People's Republic of China

^b Institute of Drug Discovery Technology, Ningbo University, Ningbo, Zhejiang
315211, People's Republic of China

* Corresponding author at: Institute of Drug Discovery Technology, Ningbo
University, Ningbo, Zhejiang 315211, People's Republic of China;

** Corresponding author at: Li Dak Sum Yip Yio Chin Kenneth Li Marine
Biopharmaceutical Research Center, Department of Marine Pharmacy, College of
Food and Pharmaceutical Sciences, Ningbo University, Ningbo, Zhejiang, 315800,
People's Republic of China.

E-mail addresses: wangning2@nbu.edu.cn (N. Wang); jinhaixiao@nbu.edu.cn (H.
Jin)

Abstract

A series of novel *N*-phenylbenzamide-4-methylamine acridine derivatives were designed and synthesized based initially on the structure of amsacrine (*m*-AMSA). Molecular docking suggested that the representative compound **9a** had affinity for binding DNA topoisomerase (Topo) II, which was comparable with that of *m*-AMSA, and furthermore that **9a** could have preferential interactions with Topo I. After synthesis of **9a** and analogues **9b-9f**, these were all tested *in vitro* and the synthesized compounds displayed potent antiproliferative activity against three different cancer cell lines (K562, CCRF-CEM and U937). Among them, compounds **9b**, **9c** and **9d** exhibiting the highest activity with IC₅₀ value ranging from 0.82 to 0.91 μM against CCRF-CEM cells. In addition, **9b** and **9d** also showed high antiproliferative activity against U937 cells, with IC₅₀ values of 0.33 and 0.23 μM, respectively. The pharmacological mechanistic studies of these compounds were evaluated by Topo I/II inhibition, western blot assay and cell apoptosis detection. In summary, **9b** effectively inhibited the activity of Topo I/II and induced DNA damage in CCRF-CEM cells and, moreover, significantly induced cell apoptosis in a concentration-dependent manner. These observations provide new information and guidance for the structural optimization of more novel acridine derivatives.

Keywords: Acridine derivatives; **Anticancer**; Topoisomerase I/II; Molecular docking; DNA damage

Cancer is expected to be **the second** leading cause of death before age 70 in most countries of the world in the 21st century, moreover, its incidence and mortality are increasing rapidly worldwide [1]. Therefore, efforts have been continuously made for the development of effective chemotherapy drugs that can have profound impacts on society through human health benefits and economic rewards. Acridine derivatives have for decades been widely explored in the field of anticancer therapeutics because of their excellent anticancer activity, especially against leukemia [2, 3]. For instance, amsacrine (*m*-AMSA) has been used clinically in a number of countries for the treatment of leukemia. Several of the coauthors have also previously developed different series of novel acridine compounds, including pyridyl acridones, benzyl acridones and 9-aminoacridine derivatives with good antitumor activity and low toxicity [4-6].

DNA topoisomerase (Topo) I/II directly regulates the topological structure of DNA and induces DNA damage by enhancing the formation of Topo I/II-DNA cleavage complexes or suppressing DNA **religation** [7]. Because of the rapid growth of tumor cells, the content and activity of Topo I and II in tumor cells are generally upregulated compared with normal cells [8]. Therefore, compared with other DNA damage agents, such as alkylating agents, topoisomerase inhibitors may have preferable anti-tumor specificity. Nowadays, a great many novel Topo I/II inhibitors with different structural scaffolds have been reported [9-11]. *m*-AMSA (**Fig. 1**) is a Topo II inhibitor with a 9-aminoacridine scaffold that has been used successfully in the treatment of acute myeloid leukemia (AML), acute lymphoblastic leukemia and acute promyelocytic leukemia [12, 13]. Specific interactions of *m*-AMSA with Topo II via the 9-anilino moiety of the drug seem to be crucial for its inhibitory activity [14]. We hypothesized that if the aniline group is not directly linked to the acridine ring, for instance, there is an intermediate chain (linker) between these two groups, the binding mode between the ligand and the protein could be affected. Based on the structure of *m*-AMSA, we designed a new representative compound **9a** with *N*-phenylbenzamide-4-methylamine acridine scaffold (**Fig. 1**).

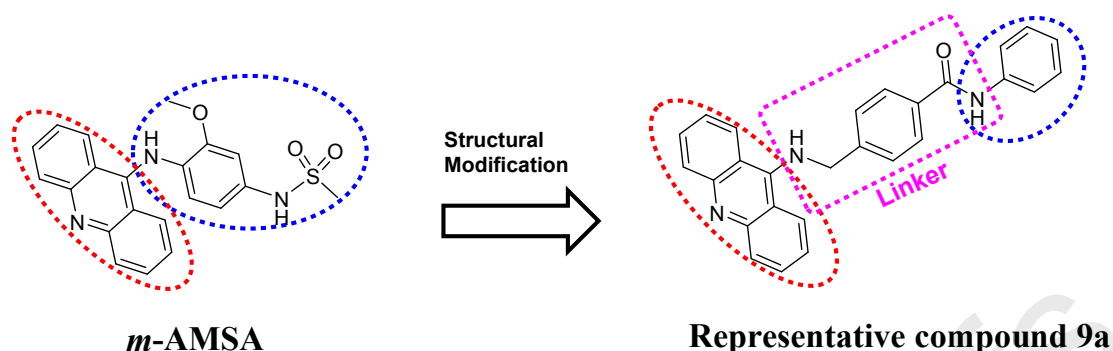


Fig. 1. the structures of *m*-AMSA and the representative compound **9a**

Molecular docking study of the *m*-AMSA and **9a** with Topo II-DNA complex mode (PDB ID: 4G0U) [15] showed that **amide NH (CONH-)** of **9a** has a hydrogen bond with Ala521, and aminomethyl NH has a hydrogen bond with Arg503 (Fig. 2A). In addition, it is important that the phenyl in **9a** (marked yellow stick) inserted into the hydrophobic pocket formed by side chain of Ile454 and Ala503 (Fig. 2B). However, the aniline side chain of *m*-AMSA (marked purple stick) could not provide such hydrophobic effect. Therefore, the strategy of introducing the extension linker between the aniline group and acridine ring is reasonable and feasible.

Since most acridine derivatives generally also have good inhibitory activity against Topo I, we also aimed to verify whether representative compound **9a** has inhibitory effect on this target. The molecular docking study (Fig. 2C) of **9a** with Topo I-DNA complex (PDB ID: 1SC7) [16] showed that **9a** had a hydrogen bond with Arg364, and the acridine ring is inserted into the cavity formed by two pairs of DNA bases. Interestingly, benzene ring was extended into hydrophobic subpocket formed by Pro431, Leu721, Lys751, Phe752 and Glu748 to form π - π and C-H- π interactions. Therefore, the above docking results indicated that this series of acridine compounds may have a Topo I/II dual inhibitory effect, which was further verified by subsequent biological experiments.

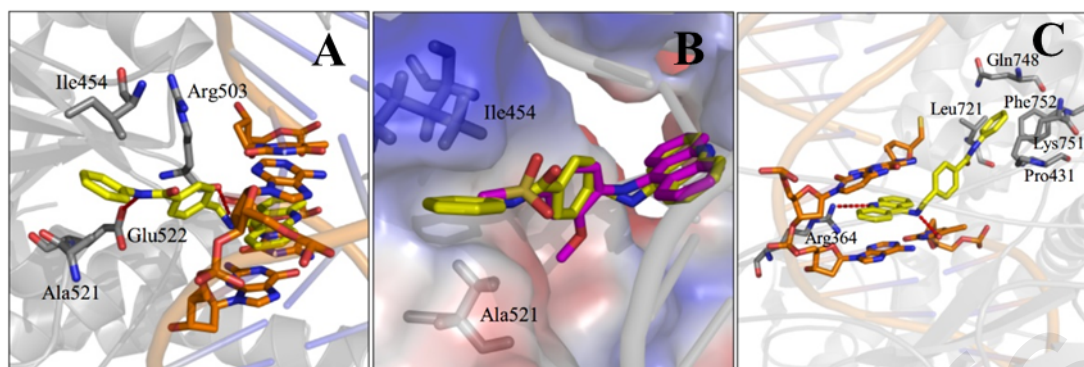
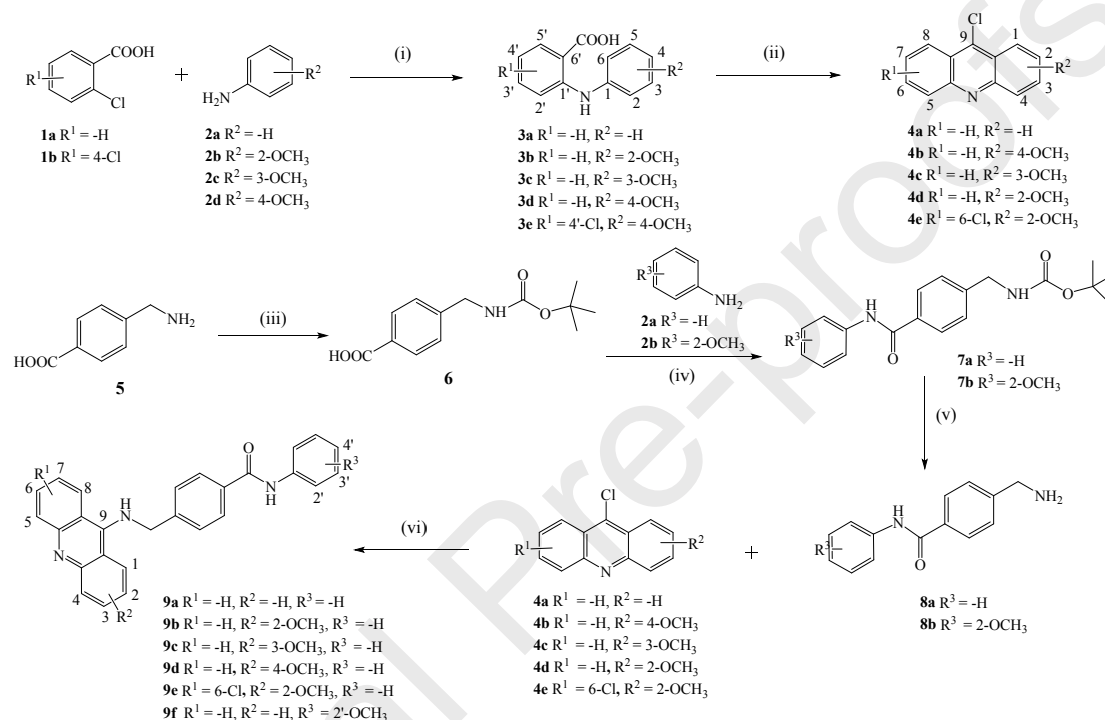


Fig. 2. Docking mode of representative compound **9a** (stick) and Topo I/II using gold 5.2.2. The carbon atom of **9a**, residues and base pairs are presented in yellow, grey and orange, respectively, the carbon atom in *m*-AMSA is colored in purple. All oxygen and nitrogen atoms are colored in red and blue respectively. Hydrogen bonds are represented by red dotted lines. (A) Topo II-**9a** binding mode; (B) Topo II-**9a** (yellow) and Topo II-*m*-AMSA (purple) binding mode; (C) Topo I-**9a** binding mode.

To investigate the relationship between the structure and activity of the target compounds, six novel *N*-phenylbenzamide-4-methylamine acridine derivatives (compounds **9a-f**) were generated preferentially by introducing different substituents on the acridine (A and C ring) and benzene (E ring) moieties. These target compounds were synthesized from the starting materials aniline and 2-chlorobenzoic acid, or its derivatives, in a sequence of chemical reactions as shown in Scheme 1. First, compounds **3a-e** were obtained in high yields from the Ullmann reaction of 2-chlorobenzoic acid **1a** or 2,4-dichlorobenzoic acid **1b** with aniline **2a** or its derivatives **2b-d** in DMF using Cu as the catalyst. Subsequent Friedel-Crafts acylation was carried out in POCl₃ for 3-5 h to give 9-chloroacridine derivatives **4a-e** [17]. The intermediate **6** was obtained in high yield by protection of the amino group of 4-(aminomethyl)benzoic acid **5**, which was carried out by reflux in methanol with BOC anhydride and triethylamine [18]. Subsequently, **6** was reacted with aniline **2a** or **2b** using *N,N'*-carbonyldiimidazole (CDI) as the condensation agent at room temperature to afford the intermediate **7a-b** [4]. 4-(aminomethyl)-*N*-phenylbenzamide **8a-b** was obtained by the hydrolysis of **7a-b** in 3M hydrochloric acid and methanol at

room temperature [19]. The desired compounds **9a-f** were produced by the nucleophilic substitution between the corresponding 9-chloroacridines **4a-e** and intermediate **8a-b** in phenol at 90-100°C under an argon atmosphere [11]. Structures of compounds were confirmed by ¹H NMR, ¹³C NMR and high resolution mass spectrometry (HR-MS) data.



Scheme 1 Reagents and conditions: (i) K₂CO₃, Cu, DMF, 130 °C, overnight; (ii) POCl₃, reflux, 3-5 h; (iii) BOC anhydride, triethylamine, methanol, reflux; (iv) CDI, DMF, overnight; (v) 3M HCl, methanol, room temperature; (vi) phenol, under the protection of N₂, 90-100 °C.

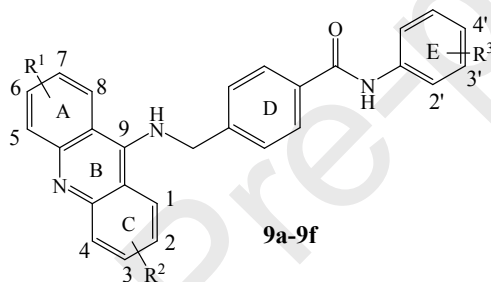
Most acridine derivatives, such as *m*-AMSA, always have been shown potential anti-leukemia activity [2]. Therefore, in this study, six *N*-phenylbenzamide-4-methylamine acridine derivatives **9a-f** and two intermediates (**4e** and **8a**) were tested against human leukemia K562 and CCRF-CEM cells by the MTT reduction assay. Furthermore, *m*-AMSA was used as the positive control. In order to study the inhibitory effect of these compounds against lymphoma cells, the

human histiocytic lymphoma cell line U937 was also selected for MTT assay screening. The structures and bioactivity testing results are summarized in Table 1. Most of the test compounds displayed potent activity against all the tested cancer cell lines, except for the intermediates **4e** and **8a** ($IC_{50} > 10 \mu M$). Among them, compounds **9b-d** exhibited the highest activity with IC_{50} value ranging from 0.82 to 0.90 μM against CCRF-CEM cells. However, the inhibitory activity of these compounds against K562 cells was relatively poor, only **9f** with methoxy substitution (R^3 group) at position 2 of the E ring had an IC_{50} value of 0.91 μM , similar to the positive control *m*-AMSA ($IC_{50} = 0.71 \mu M$). This suggested that methoxy substitution on the E ring can enhance the inhibitory activity against K562 cells. When the R^1 group on the A ring was a chlorine atom (**9e**), the antiproliferative activity against K562 and U937 cells decreased significantly, for example, the IC_{50} value of **9e** against U937 cells decreased about 6 fold compared with **9a**. When the R^2 substituent on the C ring was a methoxy group, the activity of compounds **9b-d** against CCRF-CEM cells were increased about two times compared with those without substitution (**9a** and **9f**). For instance, **9b** had significant cancer cell cytotoxic activity with IC_{50} of 0.82 μM , while the IC_{50} of **9a** was 1.56 μM . In addition, **9b** and **9d** also showed high antiproliferative activity against U937 cells, with IC_{50} values of 0.33 and 0.23 μM , respectively. This indicated that the antiproliferative activity of these compounds against U937 were significantly increased when the methoxy group was at position 2 and 4 of the C ring. In summary, the synthesized series of compounds had good antiproliferative activity against these three kinds of cancer cells. In view of the good inhibitory activity of **9b** against various tumor cells *in vitro*, it was selected for subsequent biological evaluation.

As compounds **9a-f** displayed good antiproliferative activity against K562, CCRF-CEM and U937 cells, the *in silico* predictions of drugability and pharmacokinetics of **9a-f** using Molinspiration property engine (Table 2) and BIOVIA Discovery Studio 2019 (Table 3) were performed. Lipinski's rule is often used to predict the drugability properties of small molecule drugs [20]. It can be seen from

Table 2 that the Lipinski's violations of compounds **9a-f** were 1, which are accorded with the limit of Lipinski's rule (≤ 1). The specific parameters are described as follows. For instance, the number of hydrogen bond donors and acceptors of **9b** are 2 and 5, respectively; the calculated log P (clopP) value is 5.85 (slightly higher), the molecular weight is 433.51; the number of rotatable bonds is 6, the surface area is 63.25 Å², all of which except the slightly larger clopP were within the range specified by the suggested rule. Therefore, the predicted results suggested that this series of compounds could have appropriate physicochemical and drugability properties.

Table 1 Antiproliferative activity of *N*-phenylbenzamide-4-methylamine acridines **9a-f** and two intermediates (**4e** and **8a**) against K562, CCRF-CEM and U937 cells.



Compound	R ¹	R ²	R ³	IC ₅₀ (μM)		
				CCRF-CE M	K562	U937
4e				>10	>10	>10
8a				>10	>10	>10
9a	-H	-H	-H	1.56±0.68	1.55±0.41	1.32±0.01
9b	-H	2-OCH ₃	-H	0.82±0.01	1.24±0.60	0.33±0.29
9c	-H	3-OCH ₃	-H	0.90±0.04	1.32±0.21	1.42±0.05
9d	-H	4-OCH ₃	-H	0.89±0.13	1.43±0.42	0.23±0.03
9e	6-Cl	2-OCH ₃	-H	1.30±0.06	2.37±0.56	1.80±0.84
9f	-H	-H	2'-OCH ₃	1.28±0.05	0.91±0.12	1.49±1.77
<i>m</i>-AMSA				0.03±0.01	0.71±0.09	0.08±0.01

Table 2 *In silico* prediction of physicochemical and drugability properties of **9a-f** using Molinspiration property engine v2018.10

Compound	Lipinski (≤ 1)	HBA ^a (≤ 10)	HBD ^b (≤ 5)	clogP ^c (≤ 5)	MW ^d (≤ 500)	NROTBE ^e (≤ 10)	TPSA ^f ($\leq 140\text{\AA}^2$)
9a	1	4	2	5.84	403.49	5	54.02
9b	1	5	2	5.85	433.51	6	63.25
9c	1	5	2	5.88	433.51	6	63.25
9d	1	5	2	5.88	433.51	6	63.25
9e	1	5	2	6.53	467.96	6	63.25
9f	1	5	2	5.85	433.51	6	63.25

^a Number of hydrogen-bond acceptors. ^b Number of hydrogen-bond donors. ^c Octanol/water partition coefficient. ^d Molecular weight. ^e Number of rotatable bonds. ^f Topological polar surface area.

The evaluation of predicted pharmacokinetic properties of **9a-f** were carried out using BIOVIA Discovery Studio 2019 [21]. It can be seen from Table 3 that the predicted solubility level of compounds **9a-f** is 1, indicating that the water-solubility of these compounds should be poor. However, the solubility of these compounds can be improved by converting them into counter-ionic salt forms, such as hydrochlorides. The BBB level represents blood-brain barrier permeability after oral administration, and a predicted value of 1 for **9a-f** indicated that these compounds might have high BBB permeability. Absorption Level predicts intestinal absorption after oral absorption, and the calculated values of 0 and 1 indicated that compounds **9a-f** may have good intestinal absorption characteristics. CYP2D6 Prediction refers to the prediction of enzyme inhibition of compounds **9a-f** to cytochrome P450 2D6, and “TRUE/FALSE” was used to determine whether these compounds were inhibitors of

CYP2D6. The generated data suggested that compounds **9a-f** were each unlikely to inhibit the CYP2D6 enzyme. In the analysis of a new drug, it is very important to know the basic pharmacokinetic parameters such as human plasma protein binding (PPB), and the calculated result of “TRUE” indicated that these compounds likely have high plasma protein binding rates.

Table 3 *In silico* prediction of pharmacokinetic properties of **9a-f** using BIOVIA Discovery Studio 2019

Compound	Solubility Level	BBB Level	Absorption Level	CYP2D6 Prediction	PPB Prediction
9a	1	1	0	FALSE	TRUE
9b	1	1	0	FALSE	TRUE
9c	1	1	0	FALSE	TRUE
9d	1	1	0	FALSE	TRUE
9e	1	4	1	FALSE	TRUE
9f	1	1	0	FALSE	TRUE

Molecular docking study indicated that the synthesized acridine derivatives **9a-f** had a good binding effect on Topo I/II. Therefore, it was evaluated whether these compounds could inhibit the activity of topoisomerases *in vitro*. Compounds **9a** and **9b** were selected for an enzymatic Topo I/II activity inhibition test, and camptothecin (a clinical Topo I inhibitor) and etoposide (a clinical Topo II inhibitor) were selected as positive controls for this experiment. It can be seen from Table 4 that compounds **9a** and **9b** have partial inhibitory effects on Topo I/II at 100 μ M. For example, the inhibition rate of compound **9a** on Topo I and Topo II reached 44.94% and 23.96% respectively. However, the inhibitory effects of these two compounds were not as strong as camptothecin and etoposide, respectively. Future studies should aim to optimize the structure-activity of these compounds to improve the target inhibition activity.

Table 4 The inhibitory activity of compounds **9a** and **9b** on Topo I/II

Compound	100 μ M (Inhibition rate %)	
	Topo I	Topo II
9b	7.20	17.76
9a	44.94	23.96
Camptothecin	74.32	-
Etoposide	-	40.88

“-” not tested.

When DNA damage occurs, histone H2AX is phosphorylated to form γ -H2AX, therefore γ -H2AX is considered as an important biomarker of DNA damage [22]. As a DNA damage agent, a Topo I/II inhibitor can induce DNA strand breakage and cell apoptosis. It was next determined whether compound **9b** could induce the formation of γ -H2AX by western blot analysis. For this purpose, CCRF-CEM cells were treated with **9b** with different concentration gradients. Fig. 3 shows that the content of γ -H2AX in CCRF-CEM cells was significantly increased with the increase of the concentration of **9b** from 0.5 μ M to 2 μ M.

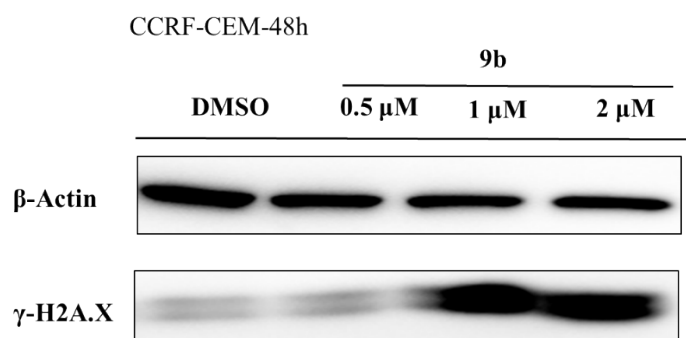


Fig. 3. 9b induced the formation of γ -H2AX *in vitro* (CCRF-CEM cells-48h)

An Annexin V-FITC/PI kit was used to detect whether compound **9b** induced apoptosis in CCRF-CEM cells. Annexin V-FITC can recognize early apoptotic cells and show green fluorescence. Propylidone iodide (PI) is used to identify late apoptotic and necrotic cells, showing red fluorescence. As can be seen from Fig. 4, **9b** can induce early apoptosis at 0.5 μ M. When the concentration of **9b** was increased to 2 μ M, the number of early apoptotic cells increased significantly. Additionally, the number of late apoptotic cells and necrotic cells also increased in a concentration-dependent manner. However, the trend was not obvious compared with early apoptotic cells. Similarly, the results obtained by using Hoechst 33342/PI kit confirmed that **9b** could significantly induce apoptosis (Fig. 1s). Hoechst 33342 can recognize apoptotic cells (blue fluorescence), and PI is used to identify necrotic cells (red fluorescence). In addition, it was observed that **9a** could also significantly induce apoptosis of CCRF-CEM cells using AnnexinV-FITC/PI apoptosis detection kit (Fig. 2s). Therefore, it is indicated that the new *N*-phenylbenzamide-4-methylamine acridine derivatives synthesized in this study were apoptosis-inducing agents.

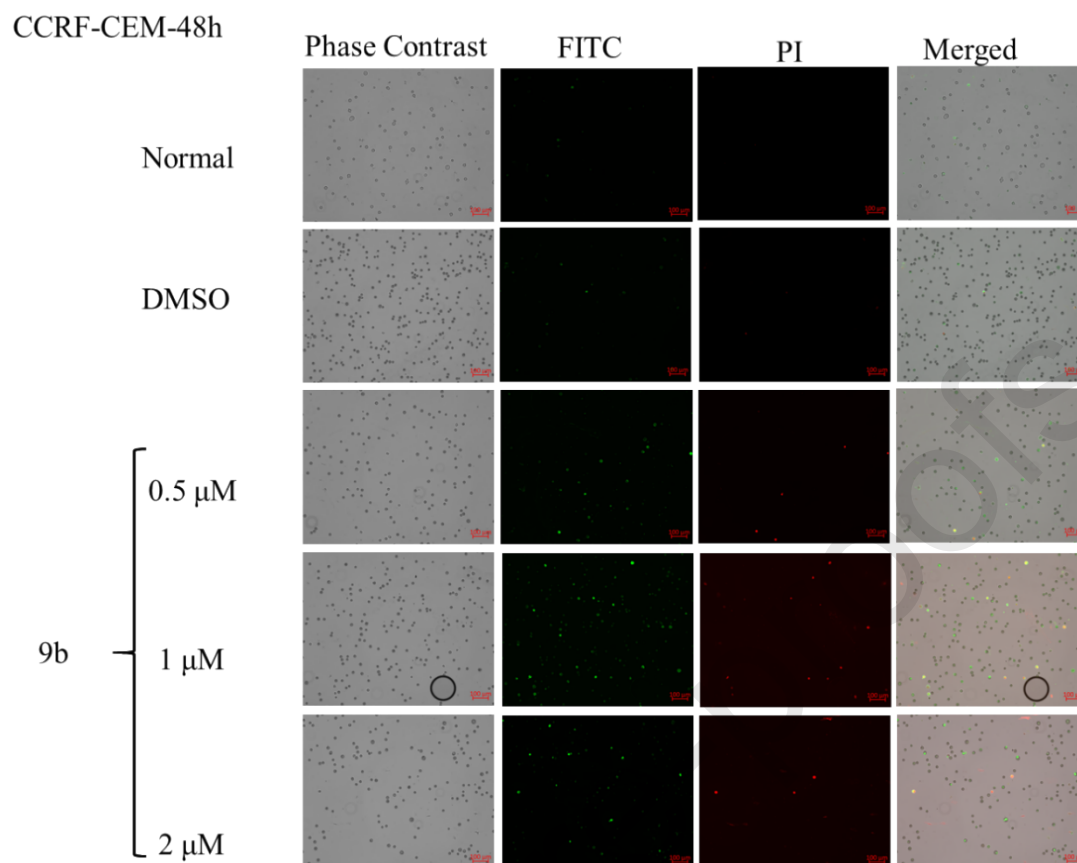


Fig. 4. **9b** induced apoptosis in CCRF-CEM cells (48h). Annexin V-FITC can recognize early apoptotic cells and show green fluorescence. PI is used to identify late apoptotic and necrotic cells, showing red fluorescence.

In this study, a series of *N*-phenylbenzamide-4-methylamine acridine derivatives (**9a-9f**) were preferentially designed and synthesized as Topo I/II inhibitors based on the structure of *m*-AMSA. MTT screening showed that these compounds exhibited good antiproliferative activity against three different cancer cell lines (K562, CCRF-CEM and U937) *in vitro*. The IC_{50} values of compound **9b** against CCRF-CEM cells and U937 cells was 0.82 and 0.33 μ M, respectively. *In silico* and *in vitro* pharmacological mechanistic studies indicated **9b** can inhibit the activity of topoisomerase I/II and induce DNA damage in CCRF-CEM cells. Moreover, **9b** induces cell apoptosis in a concentration-dependently. Accordingly, the results of this study provide new perspectives for the further structural optimization of this class of molecules for use in cancer chemotherapy research.

Acknowledgments

The authors thank the financial supports from the National Key Research and Development Program of China (2018YFC0310900), the National Natural Science Foundation of China (81850410553, 41776168), the Natural Science Foundation of Ningbo City (2018A610410), Foundation of Ningbo University for Grant (XYL18004), the National 111 Project of China (D16013), the Li Dak Sum Yip Yio Chin Kenneth Li Marine Biopharmaceutical Development Fund, and the K.C. Wong Magna Fund in Ningbo University. We appreciate Prof. C. Benjamin Naman of Ningbo University for careful editing of and thoughtful comments about the manuscript.

Appendix A. Supplementary data

Supplementary data associated with this article can be found, in the online version.

References

- [1] F. Bray, J. Ferlay, I. Soerjomataram, R. L. Siegel, L. A. Torre, A. Jemal. Global Cancer Statistics 2018: GLOBOCAN Estimates of Incidence and Mortality Worldwide for 36 Cancers in 185 Countries. *CA Cancer J. Clin.* 2018; 68: 394-424.
- [2] B. Zhang, X. Li, B. Li, C. M. Gao, Y. Y. Jiang. Acridine and its derivatives: a patent review (2009 - 2013). *Expert Opin. Ther. Pat.* 2014; 24: 647-664.
- [3] P. Belmont, J. Bosson, T. Godet, M. Tiano. Acridine and Acridone Derivatives, Anticancer Properties and Synthetic Methods: Where Are We Now? *Anti-Cancer Agent. Me.* 2007; 7: 139-169.
- [4] B. Zhang, N. Wang, C. L. Zhang, C. M. Gao, W. Zhang, K. Chen, W. B. Wu, Y. Z. Chen, C. Y. Tan, F. Liu, Y. Y. Jiang. Novel multi-substituted benzyl acridone derivatives as surviving inhibitors for hepatocellular carcinoma treatment. *Eur. J. Med. Chem.* 2017; 129: 337-348.
- [5] B. Zhang, K. Chen, N. Wang, C. M. Gao, Q. S. Sun, L. L. Li, Y. Z. Chen, C. Y.

Tan, H. X. Liu, Y. Y. Jiang. Molecular design, synthesis and biological research of novel pyridyl acridones as potent DNA-binding and apoptosis-inducing agents. *Eur. J. Med. Chem.* 2015; 93: 214-226.

[6] Z. S. Cui, X. Li, L. Li, B. Zhang, C. M. Gao, Y. Z. Chen, C. Y. Tan, H. X. Liu, W. Y. Xie, T. Yang, Y. Y. Jiang. Design, synthesis and evaluation of acridine derivatives as multi-target Src and MEK kinase inhibitors for anti-tumor treatment. *Bioorg. Med. Chem.* 2016; 24: 261-269.

[7] Y. Pommier, E. Leo, H. L. Zhang, C. Marchand. DNA topoisomerases and their poisoning by anticancer and antibacterial drugs. *Chem. Biol.* 2010; 17: 421-433.

[8] J. Kovvuri, B. Nagaraju, V. L. Nayak, R. Akunuri, M. P. N. Rao, A. Ajitha, N. Nagesh, A. Kamal. Design, synthesis and biological evaluation of new β -carboline-bisindole compounds as DNA binding, photocleavage agents and topoisomerase I inhibitors. *Eur. J. Med. Chem.* 2017; 143: 1563-1577.

[9] J. Yamaguchi, C. Ishii, N. Harada, M. Soma, H. Okamoto, M. Oitate, S. Arakawa, T. Hirai, R. Atsumi, T. Nakada, I. Hayakawa, Y. Abe, T. Agatsuma. DS-8201a, A Novel HER2-Targeting ADC with a Novel DNA Topoisomerase I Inhibitor, Demonstrates a Promising Antitumor Efficacy with Differentiation from T-DM1. *Clin. Cancer Res.* 2016; 22: 5097-5108.

[10] M. K Kathiravan, A. N Kale and S. Nilewar. Discovery and Development of Topoisomerase Inhibitors as Anticancer Agents. *Mini-rev. Med. Chem.* 2016; 16: 1219-1229.

[11] C. M. Gao, B. Li, B. Zhang, Q. S. Sun, L. L. Li, X. Li, C. J. Chen, C. Y. Tan, H. X. Liu, Y. Y. Jiang. Synthesis and biological evaluation of benzimidazole acridine derivatives as potential DNA-binding and apoptosis-inducing agents. *Bioorg. Med. Chem.* 2015; 23: 1800-1807.

[12] W. A. Denny. Acridine Derivatives as Chemotherapeutic Agents. *Curr. Med. Chem.* 2002; 9: 1655-1665.

[13] G. Escherich, K. Wos, F. Schramm, M. A. Horstmann. Amsacrine, Etoposide and Methylprednisolone As Part of the Therapy Intensification in Children with Acute

Lymphoblastic Leukemia: A Retrospective Analysis in the Trial Coall 08-09. *Blood*. 2018; 132: 5168.

[14] F. Charmantray and A. Martelli. Interest of Acridine Derivatives in the Anticancer Chemotherapy. *Curr. Pharm. Des.* 2001; 7: 1703-1724.

[15] C. C. Wu, Y. C. Li, Y. R. Wang, T. K. Li, N. L. Chan. On the structural basis and design guidelines for type II topoisomerase-targeting anticancer drugs. *Nucleic Acids Res.* 2013; 41: 10630-10640.

[16] B. L. Staker, M.D. Feese, M. Cushman, Y. Pommier, D. Zembower, L. Stewart, A. B. Burgin. Structures of Three Classes of Anticancer Agents Bound to the Human Topoisomerase I-DNA Covalent Complex. *J. Med. Chem.* 2005; 48: 2336-2346.

[17] W. Zhang, B. Zhang, W Zhang, T. Yang, N. Wang, C. M Gao, C. Y. Tan, H. X. Liu, Y. Y. Jiang. Synthesis and antiproliferative activity of 9-benzylamino-6-chloro-2-methoxy-acridine derivatives as potent DNA-binding ligands and topoisomerase II inhibitors. *Eur. J. Med. Chem.* 2016; 116: 59-70.

[18] S. W. Youn, Y. H. Kim. Pd(II)/Ag(I)-Promoted One-Pot Synthesis of Cyclic Ureas from (Hetero)Aromatic Amines and Isocyanates. *Org. Lett.* 2016; 18: 6140-6143.

[19] Y. F. Song, X. H. Huang, H. J. Hua, Q. C. Wang. The synthesis of a rigid conjugated viologen and its cucurbituril pseudorotaxanes. *Dyes Pigments*. 2017; 137: 229-235.

[20] C. A. Lipinski. Lead-and drug-like compounds: the rule-of-five revolution. *Drug Discov. Today Technol.* 2004; 1: 337-341.

[21] Dassault Systèmes BIOVIA, Discovery Studio Modeling Environment, Release 2018, San Diego: Dassault Systèmes, 2019.

[22] A. Sharma, K. Singh, A. Almasan. Histone H2AX Phosphorylation: A Marker for DNA Damage. *Methods Mol. Biol.* 2012; 920: 613-626.

Captions

Fig. 1. the structures of *m*-AMSA (A) and the representative compound **9a** (B).

Fig. 2. Docking mode of representative compound **9a** (stick) and Topo I/II using gold 5.2.2. The carbon atom of **9a**, residues and base pairs are presented in yellow, grey and orange, respectively, the carbon atom in *m*-AMSA is colored in purple. All oxygen and nitrogen atoms are colored in red and blue respectively. Hydrogen bonds are represented by red dotted lines. (A) Topo II-**9a** binding mode; (B) Topo II-**9a** (yellow) and Topo II-*m*-AMSA (purple) binding mode; (C) Topo I-**9a** binding mode.

Fig. 3. **9b** induced the formation of γ -H2AX *in vitro* (CCRF-CEM cells-48h).

Fig. 4. **9b** induced apoptosis in CCRF-CEM cells (48h). Annexin V-FITC can recognize early apoptotic cells and show green fluorescence. PI is used to identify late apoptotic and necrotic cells, showing red fluorescence.

Scheme 1 Reagents and conditions: (i) K_2CO_3 , Cu, DMF, 130 °C, overnight; (ii) $POCl_3$, reflux, 3-5 h; (iii) BOC anhydride, triethylamine, methanol, reflux; (iv) CDI, DMF, overnight; (v) 3M HCl, methanol, room temperature; (vi) phenol, under the protection of N_2 , 90-100 °C.

